冲绳海槽沉积物孔隙水地球化学特征及其指示意义

孙呈慧[1,2,5]，窦衍光[2,3*]，赵京涛[2,4]，孙治雷[2,4]，白凤龙[2,4]，

蔡峰[2,4]，李清[2,4]，翟滨[2,4]，王利波[2,4]，邹亮[2,4]

(1. 中国地质科学院, 北京 100037; 2. 中国地质调查局青岛海洋地质研究所, 山东 青岛 266237; 3. 青岛海洋科学与技术试点国家实验室 海洋地质过程与环境功能实验室, 山东 青岛 266237; 4. 青岛海洋科学与技术试点国家实验室 海洋矿产资源评价与探测技术功能实验室, 山东 青岛 266237; 5. 中国地质大学(北京), 北京 100083)

摘要： 通过对东海外陆坡–冲绳海槽 GSW1 孔沉积物孔隙水 $\delta^{13}C$、$\delta^{18}O$、$\delta^{11}B$、$\delta^{37}Cl$ 同位素和 Cl^-、SO_4^{2-}、K^+、Na^+ 等离子指标的分析，探讨了沉积物早期成岩作用、流体来源、迁移和氧化环境的变化。研究发现，GSW1 孔孔隙水溶解无机碳主要来自海水和有机质，SO_4^{2-} 浓度随深度下降比较平缓，Cl^- 浓度远低于海水，该孔表层沉积物中硫酸盐消耗主要由有机质硫酸盐还原作用（OSR）所控制，甲烷厌氧氧化作用（AOM）发生在 4 m 以下更深的层位。OSR 产生的 H_2S 向上扩散富集并被氧化，是导致 GSW1 孔 110～360 cm 处 SO_4^{2-} 浓度未明显下降的主要因素。孔隙水 SO_4^{2-} 浓度整体随着深度增加呈减小的趋势，表明 GSW1 孔沉积环境由氧化、次氧化环境逐渐转变为还原环境。$\delta^{11}B$、$\delta^{37}Cl$ 值垂向变化波动较大，一方面受到早期成岩阶段有机质降解的影响，也可能与孔隙流体扩散以及沉积物/孔隙水相互作用有关。

关键词： 硫酸盐还原；流体迁移；同位素和离子浓度；孔隙水；东海外陆坡–冲绳海槽

中图分类号： P736.4　　　　**文献标志码：** A　　　　**文章编号：** 0253-4193(2022)05-0102-11

1　引言

孔隙水是存在于固相沉积物孔隙中的液相流体。由于开放体系导致的扩散交换作用，使得海底浅表层沉积物孔隙水继承了海水组分的基本特征[1-2]，其阳离子主要包括 Na^+、K^+、Ca^{2+}、Mg^{2+}、Sr^{2+}，阴离子主要包括 Cl^-、SO_4^{2-}、Br^-、I^-、HCO_3^-（CO_3^{2-}）等。沉积物早期成岩过程发生各种物理、化学、生物反应，溶解/沉淀、吸附解析、扩散转移等过程引起沉积物孔隙水组分发生显著变化[3-5]。因此，沉积物孔隙水垂向变化特征不仅反映了被埋藏的原始溶液的性质，还反映了早期成岩过程中沉积物固液相间的化学反应和物质的交换扩散过程[6-7]。沉积物孔隙水地球化学的研究对探讨早期成岩作用、氧化还原环境变化、流体来源及运移过程、浅表层微生物地球化学过程有重要指示意义[8-13]。

目前，沉积物孔隙水地球化学已广泛应用于沉积物早期成岩作用的不同阶段。南海北部冷泉渗漏区，孔隙水化学指示了有机质硫酸盐还原作用（Organoclastic Sulfate Reduction, OSR）和甲烷厌氧氧化作用（Anaerobic Oxidation of Methane, AOM）氧化还原敏感元素的影响[14]；南海南部浅层沉积物孔隙水离子及 $\delta^{13}C_{DIC}$ 可以量化沉积物中甲烷循环[15]；马里亚纳海沟沉积物孔隙水离子反映了有氧呼吸在有机质降解的

主导作用[16]; 克罗地亚 Zrmanja 河河口半封闭海湾沉积物孔隙水化学指示了从氧化到次氧化环境的转变与有机质降解、元素的迁移规律[5]; 南开海槽俯冲带沉积物孔隙水 B 同位素地球化学揭示了流体流动与水岩相互作用[17]。

东海外陆坡–冲绳海槽是研究沉积物硫酸盐还原与甲烷厌氧氧化作用的重要区域[18–19]。研究发现,陆源沉积物的高含量为甲烷的产生提供了丰富的有机质,东海陆坡和冲绳海槽广泛发现了冷泉活动和甲烷渗漏的地质记录[20–21]。在西北斜坡发现了丰富的自生碳酸盐,与甲烷厌氧氧化作用(AOM)密切相关[22–24]。东海外陆架和冲绳海槽西部陆坡广泛发育泥火山构造、泥底辟构造[25–26],极有可能是富含甲烷的流体向上运移形成。西部陆坡广泛发育正断层为下伏含甲烷流体向上运移提供了较好的通道[27]。然而,过去对于该区域沉积物孔隙水化学研究较少[28],尤其对沉积物与早期成岩作用相关的氧化还原状态变化的关键过程认识不足,如非稳态环境下硫生物地球化学循环[29]、怎样区分 AOM 与 OSR 对硫酸盐还原的贡献[30] 等。本文选取位于东海外陆坡–冲绳海槽区域 GSW1 重力活塞沉积物样品作为研究对象,分析了其孔隙水中的 SO_4^{2-}、Cl^-、Mg^{2+}、Ca^{2+}、Sr^{2+} 以及碳、氢、氧、氯、硼同位素,研究早期成岩作用、流体来源、迁移和氧化还原环境变化。

2　区域背景

位于东海陆架外缘的冲绳海槽是西太平洋大陆边缘琉球沟–弧–盆构造体系中的边缘海盆[31]。作为连接东海与西太平洋的过渡区,冲绳海槽可以敏感的反映陆架与深海之间的环境过渡。由于远离大陆,陆源物质的供给受到限制,琉球群岛的屏障作用又使它与太平洋的联系受到影响。另一方面,海槽内存在着大量的槽底火山、地震和热液活动,加剧了沉积环境的复杂性和沉积物的多源性。黑潮及其支流是影响冲绳海槽的主要水体[32]。黑潮经台湾东北部流入冲绳海槽,并沿着东海大陆架的东部边缘向北流动,然后穿过 Tokara 海峡离开冲绳海槽,汇入北太平洋暖流[33]。黑潮对冲绳海槽以及邻近海区的海洋沉积物类型和分布特征以及古气候变化有着直接的影响。冲绳海槽及其邻近大陆的古环境演变与黑潮的变动密切相关。末次盛冰期以来,长江、黄河及台湾河流携带大量陆源物质进入冲绳海槽,巨量的陆源输入、剧烈的海平面波动、加之复杂的环流格局,使得冲绳海槽古氧化还原环境经历了明显的变化[34–36]。

冲绳海槽作为正在扩张的弧后盆地,不断接受着来自陆架区的陆源沉积物,高沉积速率有利于有机质的保存,为甲烷等烃类气体的产生提供了重要基础[25]。由于冲绳海槽是一个扩张初期的裂谷构造,地热流值高,而温度是有机质转化为烃类的重要因素。属于高热流分布区的冲绳海槽地温梯度较高,有利于烃类生成[37]。冲绳海槽经历了中新世末和上新世末两次构造运动,在北部产生了一定规模的褶皱和断层。冲绳海槽盆地中普遍发育的底辟构造、背斜构造以及网格状断裂系统,为下伏含甲烷流体向上运移创造了有利条件[38]。断裂作用和岩浆活动产生的深部热裂解气或地热流体向浅层运移,使沉积层中有机质产生热分解,有利于促进热解成因甲烷的形成[25]。丰富的陆源沉积物供应和广泛发育的正断层促使甲烷厌氧氧化过程强烈,甲烷流体运移造成该地区广泛发生甲烷渗漏活动[39–40]。

3　样品采集和分析方法

GSW1 孔是由青岛海洋地质研究所 2015 年采用"海大号"调查船在冲绳海槽中部(28°19′N, 127°21′E; 水深为 1 052.7 m)取得的重力活塞样(图 1),岩芯长度为 420 cm,共取得 36 个孔隙水样品,对其进行了离子、碳、氢、氧、氯、硼稳定同位素分析。
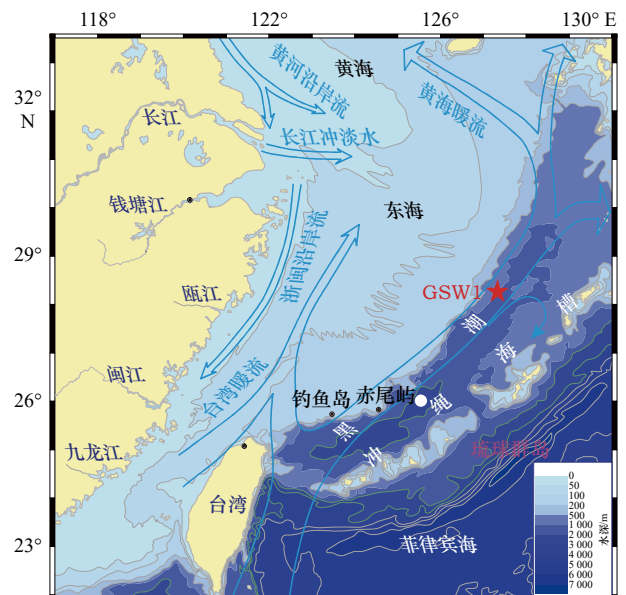

图 1　东海陆架–冲绳海槽环流体系和 GSW1 孔位置[36]

Fig. 1　Circulation system of the East China Sea outer Slope-Okinawa Trough and core GSW1 location[36]

阴离子 Cl^-、SO_4^{2-} 和阳离子 K^+、Na^+、Ca^{2+}、Mg^{2+} 浓度分析采用离子色谱法,使用仪器为日本岛津公司的 Dionex DX-100。对标准海水的重复测量表明所有

的阴离子和阳离子的标准偏差都小于 2%。测定前先用稀 HNO_3 将孔隙水稀释适当倍数,加 Rh 作为内标后上机测试,分析精度小于 10%。

碳、氧同位素($\delta^{13}C$、$\delta^{18}O$)使用 Finnigan 公司的 MAT252 进行测定。在 25℃ 条件下,先将样品与 100% 磷酸反应一段时间,然后将释放出来的 CO_2 气体送入质谱仪进行测定,$\delta^{18}O$ 和 $\delta^{13}C$ 精度均好于 0.1‰。

硼同位素($\delta^{11}B$)组成采用 Triton 热电离质谱计和基于加石墨的 $Cs_2BO_2^+$ 正热电离质谱法测定。样品装载后送入质谱仪,离子源真空抽至 $2\times10^{-7}\sim3\times10^{-7}$ Mbr 时,开始测定。分析时采用静态双接收法测定模式进行检测,获得 $R_{309/308}$ 的值。进行氧校正:$^{11}B/^{10}B = R_{309/308} -$ 0.000 79。硼同位素组成的变化用 $\delta^{11}B$ 表示,按下式计算:

$$\delta^{11}B(‰) = [(^{11}B/^{10}B)_{样品}/(^{11}B/^{10}B)_{标准} - 1]\times1\,000, \quad （1）$$

式中,标准物质是 NIST SRM 951 H_3BO_3,$(^{11}B/^{10}B)_{标准}$ 为对 NIST SRM 951 直接涂样测定的 $^{11}B/^{10}B$ 值。在仪器测定精度范围内,不同硼涂样量对 $^{11}B/^{10}B$ 比值测定没有明显的影响。硼同位素标准 NIST SRM 951 分析的外精度约为 0.2‰(2σ)。实际样品的分析外精度约为 1‰。其本次测试连续 3～5 次测定 SRM 951 的值。

氯同位素($\delta^{37}Cl$)的质谱测定是基于在石墨存在条件下检测 Cs_2Cl^+ 离子的正热电离质谱测定氯同位素的方法。样品装载后送入质谱仪,离子源真空抽至 $3\times10^{-7}\sim4\times10^{-7}$ MPa 时,开始测定。利用磁场扫描质量数为 303 和 301 的峰,利用法拉第杯和峰跳扫方式检测 303 和 301 的离子流强度,获得 303/301 的比值。因 Cs 为单同位素,其检测的 303/301 的比值即为样品中 $^{37}Cl/^{35}Cl$ 的值,无须对其进行校正。测定精度在 0.1‰ 以内。氯同位素组成的变化用 $\delta^{37}Cl$ 表示,按下式计算:

$$\delta^{37}Cl(‰) = [(^{37}Cl/^{35}Cl)_{样品}/(^{37}Cl/^{35}Cl)_{海水} - 1]\times1\,000. \quad （2）$$

4 结果

4.1 沉积物孔隙水离子垂向变化特征

GSW1 孔孔隙水离子浓度变化如图 2 所示。SO_4^{2-} 浓度在 25 cm 处略微升高,之后趋于稳定,约为 26 mmol/L。在 80～110 cm 处,SO_4^{2-} 浓度随深度增加而降低,110～360 cm 处,SO_4^{2-} 整体浓度随深度增加而升高,360 cm 以下 SO_4^{2-} 浓度急剧下降。Cl^- 浓度在上部(0～360 cm)整体浓度较为稳定,约为 550 mmol/L,继承了海水的氯值,偶有波动,在 40 cm、110 cm、140 cm 处 Cl^- 浓度下降。360 cm 以下,Cl^- 浓度开始下降,底部降到 458 mmol/L;K^+、Na^+、Ca^{2+}、Mg^{2+}、Sr^{2+} 等阳离子浓度随深度变化与 SO_4^{2-} 浓度具有相似的垂向变化特征。
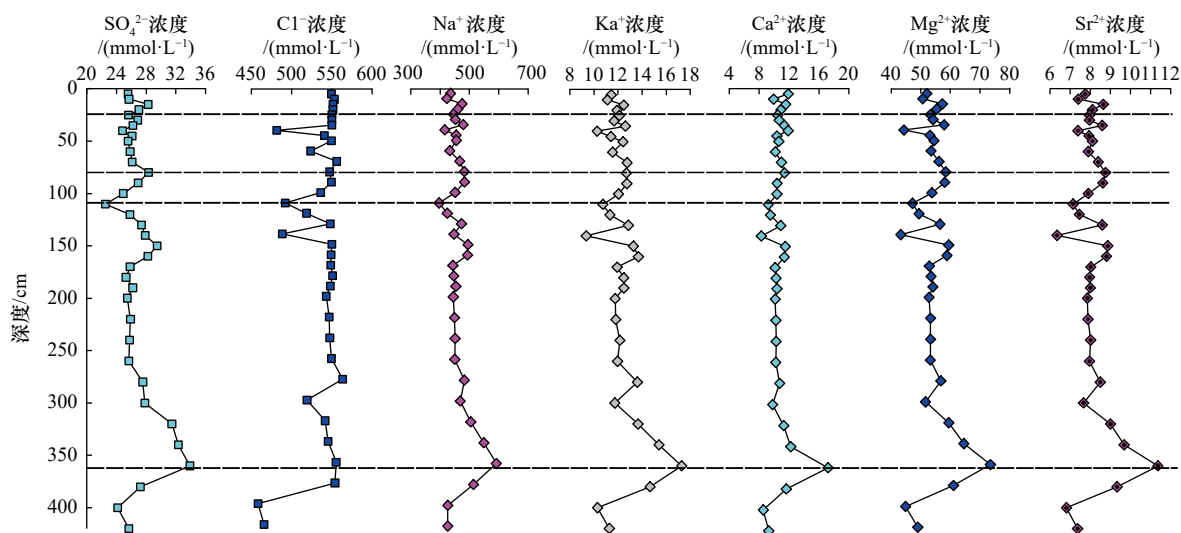
图 2　GSW1 孔沉积物孔隙水离子垂向变化

Fig. 2　Ionvertical changes of pore water in the sediments of core GSW1

4.2 沉积物孔隙水同位素垂向变化特征

GSW1 孔孔隙水同位素垂向变化如图 3 所示,$\delta^{11}B$ 值介于 36.5‰～40‰ 之间,平均值为 37.85‰,略低于正常海水(39.5‰)。$\delta^{37}Cl$ 值介于 −2‰～0‰,δD 值介于 −20‰～0‰,$\delta^{11}B$、$\delta^{37}Cl$、δD 值垂向变化较大。$\delta^{18}O$ 值为 −1.5‰～1‰ 之间,上部 0～25 cm 处,$\delta^{18}O$ 值从 −1.5‰ 增加到 −1‰,25～300 cm 处,$\delta^{18}O$ 值比较稳定,随深度缓慢增加。300 cm 以下 $\delta^{18}O$ 值显著增加,从 −0.4‰ 增加到 1‰。$\delta^{13}C$ 值均为负值,值介于 −10‰～−5‰。0～15 cm 处,$\delta^{13}C$ 值有所增加,15～50 cm
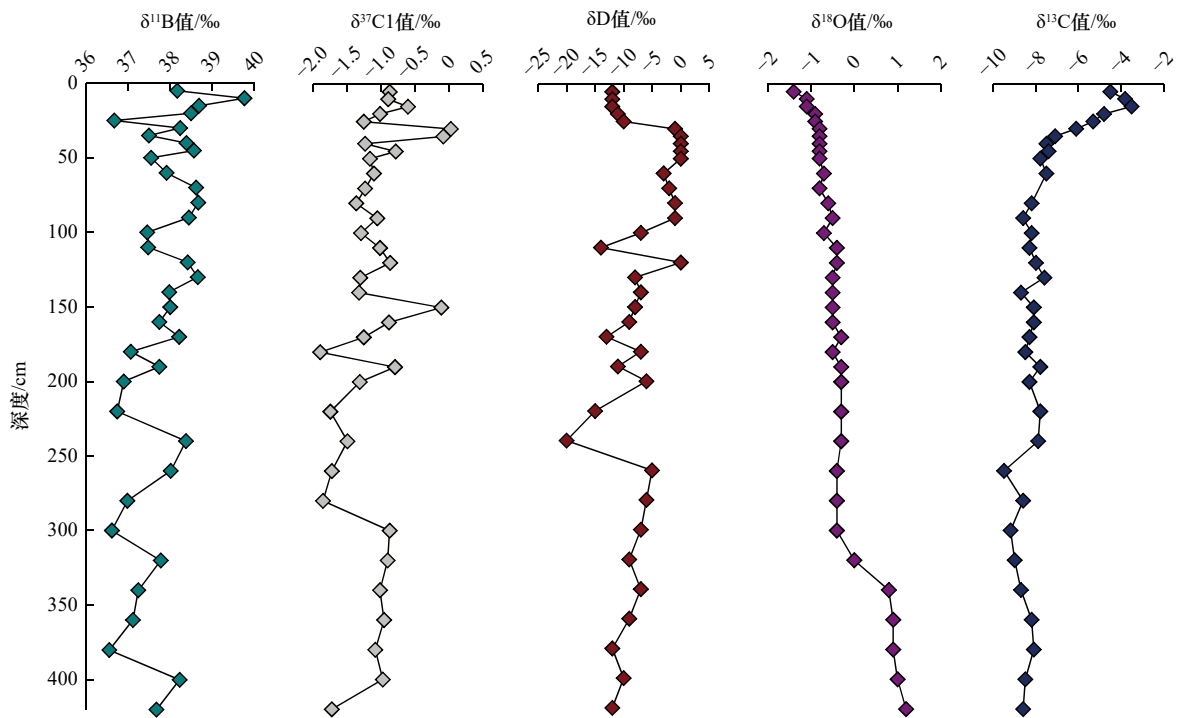
图 3   GSW1 孔沉积物孔隙水硼、氯、氢、氧、碳同位素垂向变化

Fig. 3   Vertical changes of boron, chlorine, hydrogen, oxygen, and carbon isotope in the pore water of core GSW1 sediments

处, $\delta^{13}C$ 值显著减小, 50 cm 以下, $\delta^{13}C$ 值比较稳定, 偶有波动, 随深度增加而缓慢减小。

5   讨论

5.1   离子浓度与碳氧同位素对成岩作用的指示

在早期成岩过程中, 由于沉积物中有机质对溶解氧的消耗, 沉积物孔隙水中存在自上而下的氧化–还原状态的转变, 并在不同深度出现由不同氧化剂所控制的多种不同的化学分带[41–42]。理想的化学分带由浅至深分别为有氧呼吸带、NO_3^- 还原带、Mn 还原带、Fe 还原带、硫酸盐还原带、硫酸盐–甲烷过渡带和产甲烷带[43]。

GSW1 孔 0～25 cm 处, 孔隙水中 SO_4^{2-} 浓度上升, 表明沉积物表层由于氧气作用, 有机质氧化分解, 使部分有机硫氧化形成 SO_4^{2-}。随着深度的增加, 25～80 cm 处, SO_4^{2-} 浓度几乎不变, 表明此时进入 NO_3^-、Mn、Fe 还原带, 有机硫无法氧化生成 SO_4^{2-}。之前的研究发现, 缺氧环境中, 硫酸盐还原作用是有机质厌氧矿化的主要途径之一, 所消耗的有机质占有机质氧化总量的 50% 以上[44–45]。80 cm 之下, SO_4^{2-} 浓度下降。孔隙水中 SO_4^{2-} 作为海洋沉积物中有机物再矿化的主要电子受体, 参与有机质硫酸盐还原 (OSR; 公式: $2(CH_2O)+SO_4^{2-}\rightarrow 2HCO_3^-+H_2S$)[3, 46]。此外, 甲烷厌氧氧化古菌和硫酸盐还原细菌共同作用下的甲烷厌氧氧化反应 (AOM; 公

式: $CH_4+SO_4^{2-}\rightarrow 2HCO_3^-+HS^-+H_2O$) 是缺氧沉积中早期成岩过程的另一个主要反应[47–48]。OSR 和 AOM 是海洋沉积物孔隙水中消耗 SO_4^{2-} 的主要过程。OSR 发生在硫酸盐还原带, 孔隙水中 SO_4^{2-} 浓度随深度增加逐渐被消耗, 形成一个平缓的浓度梯度。而 AOM 发生在硫酸盐还原带底部相对较薄的硫酸盐–甲烷过渡带内, 在硫酸盐甲烷界面 (Sulfate Methane Interface, SMI) 处, SO_4^{2-} 被消耗殆尽[49]。AOM 消耗 SO_4^{2-} 的速度高于 OSR, 其浓度剖面表现为梯度较大, 近似线性的特征[50–52]。GSW1 孔 SO_4^{2-} 浓度下降比较平缓, 没有呈现梯度较大, 近似线性的特征, 表明 GSW1 孔 SO_4^{2-} 消耗过程主要为 OSR 主导。此外, GSW1 孔沉积物孔隙水 Cl^- 浓度从 550 mmol/L 降到了 450 mmol/L, 低于海水的 Cl^- 浓度。孔隙水中低氯流体可能与甲烷厌氧氧化、孔隙流体混合等因素有关[53–56]。

沉积物孔隙水中溶解无机碳 (Dissolved Inorganic Carbon, DIC) 的碳同位素也是判断有机质硫酸盐还原作用 (OSR) 和甲烷厌氧氧化作用 (AOM) 的良好指标[57–59]。$\delta^{13}C$ 是判断流体碳源的重要标识, 是具有不同碳同位素值的碳源混合[60–61]。GSW1 孔孔隙水中 DIC 的潜在端元包括 3 个: 一是海水中的 DIC, DIC 可以从海水扩散到沉积物或随着沉积物埋藏过程而进入到沉积物中, 海水 $\delta^{13}C$ 值接近 0[62]; 二是沉积物有机质降解产生的 DIC, 冲绳海槽中部沉积物中有机质

$\delta^{13}C$ 值为 $-21‰$～$21.5‰$[63]；三是甲烷厌氧氧化作用产生的 DIC，甲烷来源 $\delta^{13}C$ 值小于 $-40‰$[64]。GSW1 孔沉积物孔隙水碳同位素 $\delta^{13}C$ 值在 $-10‰$～$-5‰$ 之间，随深度增加而减小，没有出现极负值。$\delta^{13}C$ 结果表明，孔隙水中 DIC 来源是海水 DIC 和有机质 DIC 两个端元混合的结果。北美布莱克海台的研究发现，SMI 界限深度为 20.5～$22.7\ m$[49-50]，南海神狐海域钻探井位的 SMI 界限深度为 17～$27\ m$[65]，南海北部东沙海区 SMI 界限深度为 6～$9\ m$[66]。由此，可以推断，GSW1 孔浅表层沉积物中硫酸盐消耗主要由有机质硫酸盐还原作用所控制，甲烷厌氧氧化作用发生在 $4\ m$ 以下的较深的层位。GSW1 孔孔隙水 $\delta^{13}C$ 值随深度增加而减小，$\delta^{18}O$ 值随深度增加而增大，两者具有明显反相关关系（图 4），这与沉积物成岩作用过程相关[67-68]。有机质还原硫酸盐过程中，硫酸根还原菌利用 SO_4^{2-} 作为电子受体进行无氧呼吸时，会产生同位素分馏，导致孔隙水中富集重同位素 ^{18}O[69-70]。$\delta^{13}C$ 和 $\delta^{18}O$ 值垂向变化的趋势，反映了硫酸盐还原反应程度不断提高，$\delta^{13}C$ 值随深度不断降低，DIC 来源于沉积物有机质降解，此时硫酸根消耗以有机质硫酸盐还原反应为主。
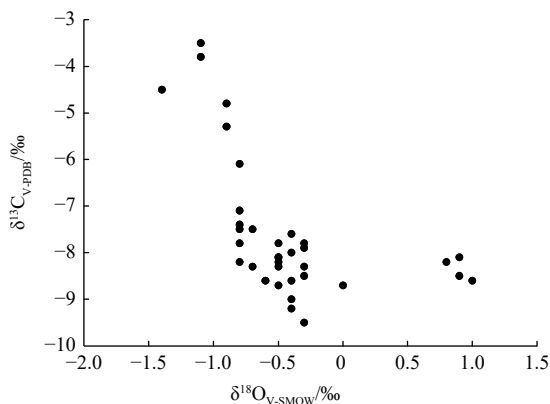

图 4　GSW1 孔沉积物孔隙水中碳氧同位素
组成的相关性

Fig. 4　Correlation between carbon isotope and oxygen isotope
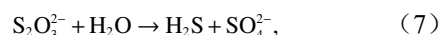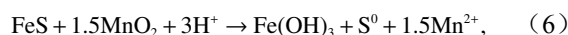in the pore water of core GSW1 sediments

OSR 发生时孔隙水中溶解的 DIC 浓度会增加，导致孔隙水中碱度升高，促进自生碳酸盐矿物的生成[71-72]。GSW1 孔沉积物孔隙水中 Ca^{2+}、Mg^{2+}、Sr^{2+} 浓度变化趋势与 SO_4^{2-} 浓度的变化趋势十分吻合，这与硫酸盐还原过程密切相关。研究发现，Ca^{2+}、Mg^{2+}、Sr^{2+} 的负异常是受到碳酸盐矿物形成的影响。在硫酸盐还原带，硫酸盐还原产生的大量 HCO_3^-（CO_3^{2-}）在孔隙水中扩散、平移，与 Ca^{2+}、Mg^{2+}、Sr^{2+} 结合形成碳酸盐沉淀[73]，使得 Ca^{2+}、Mg^{2+}、Sr^{2+} 的亏损趋势与 SO_4^{2-} 亏损几乎完全一

致。GSW1 孔 Ca^{2+}、Mg^{2+}、Sr^{2+} 浓度都出现随深度降低的趋势，表明该区有自生碳酸盐沉淀的生成。

5.2　沉积物孔隙水运移的指示

通常情况下，随着硫酸盐还原反应的进行，孔隙水中 SO_4^{2-} 浓度随深度增加而降低[74-75]。GSW1 孔孔隙水在 $80\ cm$ 处 SO_4^{2-} 浓度开始下降，说明已经进入硫酸盐还原带，SO_4^{2-} 浓度应该随深度递减，但是在 110～$350\ cm$ 段 SO_4^{2-} 浓度没有随深度递减反而是升高了，表明硫酸盐在沉积物表层的供给速率大于硫酸盐还原的消耗速率。美国俄勒冈州近海南部水合物海脊 ODP204 航次 1245 站位 $1.5\ m$ 处 SO_4^{2-} 浓度升高，略高于海水值[76]，南大西洋东部上升流地区 GeoB 3714 站位 $2\ m$ 处也出现 SO_4^{2-} 浓度升高的情况[77]，表明一些硫化物被氧化，可能与硫酸盐还原作用产生的 H_2S 在沉积物孔隙水中发生运移有关。

扩散、平流、生物扰动和灌溉是海洋沉积物早期成岩作用中孔隙水垂向运移的常见方式[46, 76-78]。沉积物受扩散和平流的影响，与上覆水体进行物质交换[48, 79]。底栖生物的扰动和灌溉可以加速含氧的海水向沉积物中运移，该过程既表现为过量的硫酸盐的输入[77]，亦导致还原产物 H_2S 在含氧带内的再氧化[76]，可以造成沉积物浅表层出现孔隙水硫酸盐浓度略高于正常海水硫酸盐浓度[78]。浅海非稳态沉积环境内，表层一定深度范围内泥质沉积物液态化，具高度流动性，受到波浪、潮流等物理过程和生物扰动等生物过程的再改造，内部沉积物强烈混合，加深了 O_2、NO_3^-、Mn^{4+} 和 Fe^{3+} 等氧化过程的深度[79-80]。活动层沉积物将保持亚氧环境并以铁锰氧化物还原为主，下伏地层产生的 H_2S 扩散到表层沉积物后被再氧化[29, 79-80]。研究表明，OSR 作用产生 H_2S 一部分向上扩散，被 O_2、铁锰氧化物等氧化为中间态（S^0、$S_2O_3^{2-}$ 等）及 SO_4^{2-}[81-82]（式（3）至式（5））。另一部分与铁氧化物反应生成铁硫化物。铁硫化物在适当的氧化剂作用下也可以被氧化为单质硫等中间产物[83-84]（式（6））。$S_2O_3^{2-}$、S^0 等是海洋沉积物中硫循环的关键中间体，可以再次还原为 H_2S，氧化为 SO_4^{2-}，或在微生物作用下发生歧化反应，同时生成 H_2S 和 SO_4^{2-}[85]（式（7）和式（8））。

$$4H_2S + 4MnO_2 \rightarrow 4S^0 + 4Mn^{2+} + 8OH^-, \quad (3)$$

$$H_2S + 7H^+ + 4FeOOH \rightarrow 0.5S_2O_3^{2-} + 6.5H_2O + 4Fe^{2+}, \quad (4)$$

$$H_2S + 4MnO_2 \rightarrow SO_4^{2-} + 4Mn^{2+} + 6OH^-, \quad (5)$$

$$FeS + 1.5MnO_2 + 3H^+ \rightarrow Fe(OH)_3 + S^0 + 1.5Mn^{2+}, \quad (6)$$

$$S_2O_3^{2-} + H_2O \rightarrow H_2S + SO_4^{2-}, \quad (7)$$

$$4S^0 + 4H_2O \rightarrow 3H_2S + SO_4^{2-} + 2H^+. \quad (8)$$
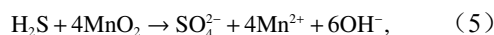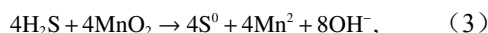
东海陆坡紧邻冲绳海槽，是中国大陆和台湾陆源

沉积物向冲绳海槽输运的过渡区。前人研究发现东海陆坡存在小型滑塌沉积[86]。GSW1 孔 110～360 cm 处 SO_4^{2-} 浓度未明显下降反而升高,可能是在浅海非稳态沉积环境内,由于受到滑塌、波浪等物理再改造和生物扰动作用,导致有机质硫酸盐还原产生的 H_2S 向上扩散富集、被再氧化。在 150 cm 和 360 cm 处 SO_4^{2-} 浓度显著升高可能是该处 H_2S 富集强烈。在此深度下沉积物中没有溶解的 O_2,所以氧化必须是厌氧的,氧化剂可能为铁锰氧化物。H_2S 的产生对于早期成岩作用中沉积物的氧化还原状态产生重要影响。H_2S 在沉积物孔隙水中富集,可能使沉积物中的硫酸盐还原带变浅,引起整个区域环境趋向还原[14]。孔隙水 SO_4^{2-} 浓度整体随着深度的增加而减小表明沉积环境由氧化、次氧化环境逐渐转变为还原环境。

5.3　孔隙水硼、氯同位素赋存机制与指示意义

孔隙水中的 B 和 $\delta^{11}B$ 可以提供流体来源、有机质降解以及甲烷水合物形成的关键信息,因此是评估不同深度的流体迁移和沉积物/水相互作用的敏感示踪剂[87−90]。

GSW1 孔沉积物孔隙水 $\delta^{11}B$ 值在 36.5‰～40‰ 之间,与全球海水 $\delta^{11}B$ 平均值 39.5‰ 相近[91−92],与 $\delta^{11}B$ 的其他端元值相差较远(沉积物可交换态、晶格结合态、海洋碳酸盐 $\delta^{11}B$ 值分别为+15‰、−5‰～−10‰、−20‰)[93−95],表明孔隙水 $\delta^{11}B$ 值主要来自海水。以往研究发现,沉积物中黏土矿物优先吸附 ^{10}B,这个过程会导致孔隙水中 B 耗尽、^{11}B 富集[93],浅海沉积物孔隙水的 B 浓度通常随着深度增加而减小,而 $\delta^{11}B$ 值则增加。而沉积物中 $\delta^{11}B$ 值的下降,一般是由于沉积物中由黏土矿物的释放出富 ^{10}B 的流体造成的[95]。GSW1 孔自上至下 $\delta^{11}B$ 值波动显著,且有缓慢降低趋势(图 3)。$\delta^{11}B$ 值下降表明 GSW1 孔黏土矿物吸附作用并不明显,硫酸盐还原作用有机物分解可能是主要原因[95−96];

另一方面,$\delta^{11}B$ 值上下显著波动,可能与硫酸盐还原作用产生的 H_2S 导致沉积物中孔隙水发生上下迁移、不同 $\delta^{11}B$ 值相互混合有关。GSW1 孔孔隙水 $\delta^{37}Cl$ 值垂向同样波动较大,发生了显著的分馏。氯同位素偏负可能与流体扩散作用有关,含氯流体的沉淀、解离和蒸发将导致固相中 ^{37}Cl 的富集[97−98];也可能是由沉积物成岩过程中矿物和孔隙水的相互作用引起[99−100]。

6　结论

(1)东海外陆坡−冲绳海槽 GSW1 孔 SO_4^{2-} 消耗主要由有机质硫酸盐还原控制。$\delta^{13}C$ 和 $\delta^{18}O$ 值的垂向变化趋势,反映了 OSR 反应程度不断提高,$\delta^{13}C$ 值随深度不断降低,溶解的 DIC 来源于沉积物有机质降解。Ca^{2+}、SO_4^{2-}、Mg^{2+} 出现负异常并与 SO_4^{2-} 亏损一致表明与硫酸盐还原反应有关,该区有自生碳酸盐沉淀生成。GSW1 孔甲烷厌氧氧化发生在 4 m 以下的较深层位。

(2)GSW1 孔 110 cm 处 SO_4^{2-} 升高与 H_2S 在孔隙水中扩散迁移有关。OSR 还原过程产生的 H_2S,H_2S 往上迁移被再次氧化为硫中间体或 SO_4^{2-},造成 GSW1 孔 SO_4^{2-} 浓度升高,同时使钻孔环境趋向还原。孔隙水 SO_4^{2-} 浓度整体随着深度的增加而减小的趋势,表明 GSW1 孔沉积环境由氧化、次氧化环境逐渐转变为还原环境。

(3)GSW1 孔 $\delta^{11}B$ 值比海水轻,黏土矿物吸附作用并不明显,可能是与硫酸盐还原作用有机物分解有关。$\delta^{11}B$ 和 ^{37}Cl 值上下显著波动,可能与硫酸盐还原作用产生的 H_2S 使得孔隙水发生上下迁移有关,另一方面,沉积物成岩过程中矿物和孔隙水的相互作用也可能是影响 $\delta^{11}B$ 和 ^{37}Cl 组成的重要因素。

参考文献:

[1]　Chester R. Marine Geochemistry[M]. 2nd ed. Netherlands: Springer, 1990: 4−5.

[2]　Hoefs J. 稳定同位素地球化学[M]. 北京: 海洋出版社, 2002: 144−145.
　　　Hoefs J. Stable Isotope Geochemistry[M]. Beijing: China Ocean Press, 2002: 144−145.

[3]　Berner R A. Early Diagenesis: A Theoretical Approach[M]. New Jersey: Princeton University Press, 1980.

[4]　Beck M, Dellwig O, Schnetger B, et al. Cycling of trace metals (Mn, Fe, Mo, U, V, Cr) in deep pore waters of intertidal flat sediments[J]. Geochimica et Cosmochimica Acta, 2008, 72(12): 2822−2840.

[5]　Fiket Ž, Fiket T, Ivanić M, et al. Pore water geochemistry and diagenesis of estuary sediments—an example of the Zrmanja River Estuary (Adriatic coast, Croatia)[J]. Journal of Soils and Sediments, 2019, 19(4): 2048−2060.

[6]　Bianchi T S. Geochemistry of Marine Sediments[M]. Princeton: Princeton University Press, 2006.

[7]　Wang Xiaojing, Li Li, Liu Jihua, et al. Early diagenesis of redox-sensitive trace metals in the northern Okinawa Trough[J]. Acta Oceanologica Sinica, 2019, 38(12): 14−25.

[8]　Chatterjee S, Dickens G R, Bhatnagar G, et al. Pore water sulfate, alkalinity, and carbon isotope profiles in shallow sediment above mar-

ine gas hydrate systems: a numerical modeling perspective[J]. Journal of Geophysical Research: Solid Earth, 2011, 116(B9): B09103.

[9]   Treude T, Krause S, Maltby J, et al. Sulfate reduction and methane oxidation activity below the sulfate-methane transition zone in Alaskan Beaufort Sea continental margin sediments: implications for deep sulfur cycling[J]. Geochimica et Cosmochimica Acta, 2014, 144: 217−237.

[10]   Pellerin A, Antler G, Røy H, et al. The sulfur cycle below the sulfate-methane transition of marine sediments[J]. Geochimica et Cosmochimica Acta, 2018, 239: 74−89.

[11]   Zindorf M, März C, Wagner T, et al. Deep sulfate-methane-transition and sediment diagenesis in the Gulf of Alaska (IODP Site U1417)[J]. Marine Geology, 2019, 417: 105986.

[12]   Hu Yu, Feng Dong, Peckmann J, et al. The impact of diffusive transport of methane on pore-water and sediment geochemistry constrained by authigenic enrichments of carbon, sulfur, and trace elements: a case study from the Shenhu area of the South China Sea[J]. Chemical Geology, 2020, 553: 119805.

[13]   Hong W L, Pape T, Schmidt C, et al. Interactions between deep formation fluid and gas hydrate dynamics inferred from pore fluid geochemistry at active pockmarks of the Vestnesa Ridge, west Svalbard margin[J]. Marine and Petroleum Geology, 2021, 127: 104957.

[14]   Hu Yu, Feng Dong, Liang Qianyong, et al. Impact of anaerobic oxidation of methane on the geochemical cycle of redox-sensitive elements at cold-seep sites of the northern South China Sea[J]. Deep-Sea Research Part II: Topical Studies in Oceanography, 2015, 122: 84−94.

[15]   Feng Junxi, Yang Shengxiong, Liang Jinqiang, et al. Methane seepage inferred from the porewater geochemistry of shallow sediments in the Beikang Basin of the southern South China Sea[J]. Journal of Asian Earth Sciences, 2018, 168: 77−86.

[16]   Liu Shuangquan, Peng Xiaotong. Organic matter diagenesis in hadal setting: insights from the pore-water geochemistry of the Mariana Trench sediments[J]. Deep-Sea Research Part I: Oceanographic Research Papers, 2019, 147: 22−31.

[17]   Hüpers A, Kasemann S A, Kopf A J, et al. Fluid flow and water-rock interaction across the active Nankai Trough subduction zone fore-arc revealed by boron isotope geochemistry[J]. Geochimica et Cosmochimica Acta, 2016, 193: 100−118.

[18]   Xu Cuiling, Wu Nengyou, Sun Zhilei, et al. Methane seepage inferred from pore water geochemistry in shallow sediments in the western slope of the mid-Okinawa Trough[J]. Marine and Petroleum Geology, 2018, 98: 306−315.

[19]   Xu Cuiling, Wu Nengyou, Sun Zhilei, et al. Assessing methane cycling in the seep sediments of the mid-Okinawa Trough: insights from pore-water geochemistry and numerical modeling[J]. Ore Geology Reviews, 2021, 129: 103909.

[20]   Sun Zhilei, Wu Nengyou, Cao Hong, et al. Hydrothermal metal supplies enhance the benthic methane filter in oceans: an example from the Okinawa Trough[J]. Chemical Geology, 2019, 525: 190−209.

[21]   Cao Hong, Sun Zhilei, Wu Nengyou, et al. Mineralogical and geochemical records of seafloor cold seepage history in the northern Okinawa Trough, East China Sea[J]. Deep-Sea Research Part I: Oceanographic Research Papers, 2020, 155: 103165.

[22]   Sun Zhilei, Wei Helong, Zhang Xunhua, et al. A unique Fe-rich carbonate chimney associated with cold seeps in the Northern Okinawa Trough, East China Sea[J]. Deep-Sea Research Part I: Oceanographic Research Papers, 2015, 95: 37−53.

[23]   Peng Xiaotong, Guo Zixiao, Chen Shun, et al. Formation of carbonate pipes in the northern Okinawa Trough linked to strong sulfate exhaustion and iron supply[J]. Geochimica et Cosmochimica Acta, 2017, 205: 1−13.

[24]   Li Jiwei, Peng Xiaotong, Bai Shijie, et al. Biogeochemical processes controlling authigenic carbonate formation within the sediment column from the Okinawa Trough[J]. Geochimica et Cosmochimica Acta, 2018, 222: 363−382.

[25]   Xu Ning, Wu Shiguo, Shi Buqing, et al. Gas hydrate associated with mud diapirs in southern Okinawa Trough[J]. Marine and Petroleum Geology, 2009, 26(8): 1413−1418.

[26]   Xing Junhui, Jiang Xiaodian, Li Deyong. Seismic study of the mud diapir structures in the Okinawa Trough[J]. Geological Journal, 2016, 51(S1): 203−208.

[27]   Yin Ping, Berné S, Vagner P, et al. Mud volcanoes at the shelf margin of the East China Sea[J]. Marine Geology, 2003, 194(3/4): 135−149.

[28]   李清, 蔡峰, 梁杰, 等. 东海冲绳海槽西部陆坡甲烷渗漏发育的孔隙水地球化学证据[J]. 中国科学: 地球科学, 2015, 58(6): 986−995.
        Li Qing, Cai Feng, Liang Jie, et al. Geochemical constraints on the methane seep activity in western slope of the middle Okinawa Trough, the East China Sea[J]. Science China Earth Sciences, 2015, 58(6): 986−995.

[29]   刘喜停, 李安春, 马志鑫, 等. 沉积过程对自生黄铁矿硫同位素的约束[J]. 沉积学报, 2020, 38(1): 124−137.
        Liu Xiting, Li Anchun, Ma Zhixin, et al. Constraint of sedimentary processes on the sulfur isotope of authigenic pyrite[J]. Acta Sedimentologica Sinica, 2020, 38(1): 124−137.

[30]   Jørgensen B B, Beulig F, Egger M, et al. Organoclastic sulfate reduction in the sulfate-methane transition of marine sediments[J]. Geochimica et Cosmochimica Acta, 2019, 254: 231−245.

[31]   Sibuet J C, Deffontaines B, Hsu S K, et al. Okinawa Trough backarc basin: early tectonic and magmatic evolution[J]. Journal of Geophysical Research: Solid Earth, 1998, 103(B12): 30245−30267.

[32]   余华. 冲绳海槽中部37 Cal ka BP以来的古气候和古海洋环境研究[D]. 青岛: 中国海洋大学, 2006.
        Yu Hua. Paleoclimate and paleoceanography study of the middle Okinawa Trough in the last 37 Cal ka BP[D]. Qingdao: Ocean University of China, 2006.

[33] Yang Dezhou, Yin Baoshu, Liu Zhiliang, et al. Numerical study of the ocean circulation on the East China Sea shelf and a Kuroshio bottom branch northeast of Taiwan in summer[J]. Journal of Geophysical Research: Oceans, 2011, 116(C5): C05015.

[34] Kao S J, Horng C S, Hsu S C, et al. Enhanced deepwater circulation and shift of sedimentary organic matter oxidation pathway in the Okinawa Trough since the Holocene[J]. Geophysical Research Letters, 2005, 32(15): L15609.

[35] Kao S J, Wu C R, Hsin Y C, et al. Effects of sea level change on the upstream Kuroshio Current through the Okinawa Trough[J]. Geophysical Research Letters, 2006, 33(16): L16604.

[36] Dou Yanguang, Yang Shouye, Li Chao, et al. Deepwater redox changes in the southern Okinawa Trough since the last glacial maximum[J]. Progress in Oceanography, 2015, 135: 77−90.

[37] 栾锡武, 秦蕴珊, 张训华, 等. 东海陆坡及相邻槽底天然气水合物的稳定域分析[J]. 地球物理学报, 2003, 46(4): 467−475.
Luan Xiwu, Qin Yunshan, Zhang Xunhua, et al. The stability zone of gas hydrate in the slope of East China Sea and neighboring trough basin area[J]. Chinese Journal of Geophysics, 2003, 46(4): 467−475.

[38] 栾锡武, 鲁银涛, 赵克斌, 等. 东海陆坡及邻近槽底天然气水合物成藏条件分析及前景[J]. 现代地质, 2008, 22(3): 342−355.
Luan Xiwu, Lu Yintao, Zhao Kebin, et al. Geological factors for the development and newly advances in exploration of gas hydrate in East China Sea slope and Okinawa Trough[J]. Geoscience, 2008, 22(3): 342−355.

[39] 李清, 蔡峰, 闫桂京, 等. 东海冲绳海槽泥火山发育区甲烷气体来源研究[J]. 海洋地质前沿, 2020, 36(9): 79−86.
Li Qing, Cai Feng, Yan Guijing, et al. Origin of pore water methane recovered from mud volcanos in the Okinawa Trough[J]. Marine Geology Frontiers, 2020, 36(9): 79−86.

[40] Li Qing, Cai Feng, Yan Guijing, et al. Widespread methane seep activities along the western slope of the Okinawa Trough, East China Sea[J]. Acta Geologica Sinica (English Edition), 2017, 91(4): 1505−1506.

[41] 李超, 程猛, Algeo T J, 等. 早期地球海洋水化学分带的理论预测[J]. 中国科学: 地球科学, 2015, 58(11): 1901−1909.
Li Chao, Cheng Meng, Algeo T J, et al. A theoretical prediction of chemical zonation in early oceans (>520 Ma)[J]. Science China Earth Sciences, 2015, 58(11): 1901−1909.

[42] Jørgensen B B, Kasten S. Sulfur cycling and methane oxidation[M]//Schulz H D, Zabel M. Marine Geochemistry. Berlin, Heidelberg: Springer, 2006: 271−309.

[43] Canfield D E, Thamdrup B. Towards a consistent classification scheme for geochemical environments, or, why we wish the term 'suboxic' would go away[J]. Geobiology, 2009, 7(4): 385−392.

[44] Jørgensen B B. Mineralization of organic matter in the sea bed-the role of sulphate reduction[J]. Nature, 1982, 296(5858): 643−645.

[45] 朱茂旭, 史晓宁, 杨桂朋, 等. 海洋沉积物中有机质早期成岩矿化路径及其相对贡献[J]. 地球科学进展, 2011, 26(4): 355−364.
Zhu Maoxu, Shi Xiaoning, Yang Guipeng, et al. Relative contributions of various early diagenetic pathways to mineralization of organic matter in marine sediments: an overview[J]. Advances in Earth Science, 2011, 26(4): 355−364.

[46] Jørgensen B B, Weber A, Zopfi J. Sulfate reduction and anaerobic methane oxidation in Black Sea sediments[J]. Deep-Sea Research Part I: Oceanographic Research Papers, 2001, 48(9): 2097−2120.

[47] Boetius A, Ravenschlag K, Schubert C J, et al. A marine microbial consortium apparently mediating anaerobic oxidation of methane[J]. Nature, 2000, 407(6804): 623−626.

[48] Jørgensen B B, Böttcher M E, Lüschen H, et al. Anaerobic methane oxidation and a deep H₂S sink generate isotopically heavy sulfides in Black Sea sediments[J]. Geochimica et Cosmochimica Acta, 2004, 68(9): 2095−2118.

[49] Borowski W S, Paull C K, Ussler III W. Global and local variations of interstitial sulfate gradients in deep-water, continental margin sediments: sensitivity to underlying methane and gas hydrates[J]. Marine Geology, 1999, 159(1/4): 131−154.

[50] Borowski W S, Paull C K, Ussler III W. Marine pore-water sulfate profiles indicate in situ methane flux from underlying gas hydrate[J]. Geology, 1996, 24(7): 655−658.

[51] Dickens G R. Sulfate profiles and barium fronts in sediment on the Blake Ridge: present and past methane fluxes through a large gas hydrate reservoir[J]. Geochimica et Cosmochimica Acta, 2001, 65(4): 529−543.

[52] Yang Tao, Jiang Shaoyong, Ge Lu, et al. Geochemical characteristics of pore water in shallow sediments from Shenhu area of South China Sea and their significance for gas hydrate occurrence[J]. Chinese Science Bulletin, 2010, 55(8): 752−760.

[53] Toki T, Tsunogai U, Gamo T, et al. Detection of low-chloride fluids beneath a cold seep field on the Nankai accretionary wedge off Kumano, south of Japan[J]. Earth and Planetary Science Letters, 2004, 228(1/2): 37−47.

[54] Torres M E, Wallmann K, Tréhu A M, et al. Gas hydrate growth, methane transport, and chloride enrichment at the southern summit of hydrate ridge, Cascadia margin off Oregon[J]. Earth and Planetary Science Letters, 2004, 226(1/2): 225−241.

[55] Luo Min, Chen Linying, Tong Hongpeng, et al. Gas hydrate occurrence inferred from dissolved Cl⁻ concentrations and δ¹⁸O values of pore water and dissolved sulfate in the shallow sediments of the pockmark field in southwestern Xisha Uplift, northern South China Sea[J]. Energies, 2014, 7(6): 3886−3899.

[56] Wallmann K, Riedel M, Hong Weili, et al. Gas hydrate dissociation off Svalbard induced by isostatic rebound rather than global warming[J]. Nature Communications, 2018, 9(1): 83.

[57] Yang Tao, Jiang Shaoyong, Yang Jinghong, et al. Dissolved inorganic carbon (DIC) and its carbon isotopic composition in sediment pore waters from the Shenhu area, northern South China Sea[J]. Journal of Oceanography, 2008, 64(2): 303−310.

[58] Chen Yifeng, Ussler III W, Haflidason H, et al. Sources of methane inferred from pore-water δ^{13}C of dissolved inorganic carbon in Pockmark G11, offshore Mid-Norway[J]. Chemical Geology, 2010, 275(3/4): 127−138.

[59] Luo Min, Chen Linying, Wang Shuhong, et al. Pockmark activity inferred from pore water geochemistry in shallow sediments of the pockmark field in southwestern Xisha Uplift, northwestern South China Sea[J]. Marine and Petroleum Geology, 2013, 48: 247−259.

[60] Mazzini A, Ivanov M K, Parnell J, et al. Methane-related authigenic carbonates from the Black Sea: geochemical characterisation and relation to seeping fluids[J]. Marine Geology, 2004, 212(1/4): 153−181.

[61] Kastner M, Claypool G, Robertson G. Geochemical constraints on the origin of the pore fluids and gas hydrate distribution at Atwater Valley and Keathley Canyon, northern Gulf of Mexico[J]. Marine and Petroleum Geology, 2008, 25(9): 860−872.

[62] 杨杰东, 徐士进. 同位素与全球环境变化[M]. 北京: 地质出版社, 2007: 62−64.
Yang Jiedong, Xu Shijin. Isotopes and Global Environmental Changes[M]. Beijing: Geological Press, 2007: 62−64.

[63] Kao S J, Roberts A P, Hsu S C, et al. Monsoon forcing, hydrodynamics of the Kuroshio Current, and tectonic effects on sedimentary carbon and sulfur cycling in the Okinawa Trough since 90 ka[J]. Geophysical Research Letters, 2006, 33(5): L05610.

[64] Chuang Peichuan, Yang T F, Wallmann K, et al. Carbon isotope exchange during anaerobic oxidation of methane (AOM) in sediments of the northeastern South China Sea[J]. Geochimica et Cosmochimica Acta, 2019, 246: 138−155.

[65] 吴能友, 张海啟, 杨胜雄, 等. 南海神狐海域天然气水合物成藏系统初探[J]. 天然气工业, 2007, 27(9): 1−6.
Wu Nengyou, Zhang Haiqi, Yang Shengxiong, et al. Preliminary discussion on natural gas hydrate (NGH) reservoir system of Shenhu area, north slope of South China Sea[J]. Natural Gas Industry, 2007, 27(9): 1−6.

[66] 陆红锋, 刘坚, 陈芳, 等. 南海东北部硫酸盐还原−甲烷厌氧氧化界面——海底强烈甲烷渗溢的记录[J]. 海洋地质与第四纪地质, 2012, 32(1): 93−98.
Lu Hongfeng, Liu Jian, Chen Fang, et al. Shallow sulfate-methane interface in northeastern South China Sea: an indicator of strong methane seepage on seafloor[J]. Marine Geology & Quaternary Geology, 2012, 32(1): 93−98.

[67] Suess E. Marine cold seeps and their manifestations: geological control, biogeochemical criteria and environmental conditions[J]. International Journal of Earth Sciences, 2014, 103(7): 1889−1916.

[68] 杨克红, 于晓果, 初凤友, 等. 南海北部甲烷渗漏系统环境变化的碳、氧同位素记录[J]. 地球科学, 2016, 41(7): 1206−1215.
Yang Kehong, Yu Xiaoguo, Chu Fengyou, et al. Environmental changes in methane seeps recorded by carbon and oxygen isotopes in the northern South China Sea[J]. Earth Science, 2016, 41(7): 1206−1215.

[69] Antler G, Turchyn A V, Herut B, et al. A unique isotopic fingerprint of sulfate-driven anaerobic oxidation of methane[J]. Geology, 2015, 43(7): 619−622.

[70] Antler G, Turchyn A V, Rennie V, et al. Coupled sulfur and oxygen isotope insight into bacterial sulfate reduction in the natural environment[J]. Geochimica et Cosmochimica Acta, 2013, 118: 98−117.

[71] Peckmann J, Thiel V. Carbon cycling at ancient methane-seeps[J]. Chemical Geology, 2004, 205(3/4): 443−467.

[72] Snyder G T, Hiruta A, Matsumoto R, et al. Pore water profiles and authigenic mineralization in shallow marine sediments above the methane-charged system on Umitaka Spur, Japan Sea[J]. Deep-Sea Research Part II: Topical Studies in Oceanography, 2007, 54(11/13): 1216−1239.

[73] Peckmann J, Reimer A, Luth U, et al. Methane-derived carbonates and authigenic pyrite from the northwestern Black Sea[J]. Marine Geology, 2001, 177(1/2): 129−150.

[74] Hensen C, Zabel M, Pfeifer K, et al. Control of sulfate pore-water profiles by sedimentary events and the significance of anaerobic oxidation of methane for the burial of sulfur in marine sediments[J]. Geochimica et Cosmochimica Acta, 2003, 67(14): 2631−2647.

[75] Bowles M W, Samarkin V A, Bowles K M, et al. Weak coupling between sulfate reduction and the anaerobic oxidation of methane in methane-rich seafloor sediments during *ex situ* incubation[J]. Geochimica et Cosmochimica Acta, 2011, 75(2): 500−519.

[76] Claypool G E, Milkov A V, Lee Y J, et al. Microbial methane generation and gas transport in shallow sediments of an accretionary complex, southern hydrate ridge (ODP Leg 204), offshore Oregon, USA[J]. Proceedings of the Ocean Drilling Program Scientific Results, 2006, 204: 1−52.

[77] Fossing H, Ferdelman T G, Berg P. Sulfate reduction and methane oxidation in continental margin sediments influenced by irrigation (South-East Atlantic off Namibia)[J]. Geochimica et Cosmochimica Acta, 2000, 64(5): 897−910.

[78] 刘晨晖. 海洋天然气水合物区硫酸盐−甲烷过渡带铁、硫组分和硫同位素地球化学研究[D]. 南京: 南京大学, 2016.
Liu Chenhui. A study of iron and sulfur species and sulfur isotope geochemistry in marine sediments from gas hydrate-bearing regions: implications for sulfate-methane transition zone[D]. Nanjing: Nanjing University, 2016.

[79] Aller R C, Madrid V, Chistoserdov A, et al. Unsteady diagenetic processes and sulfur biogeochemistry in tropical deltaic muds: implications for oceanic isotope cycles and the sedimentary record[J]. Geochimica et Cosmochimica Acta, 2010, 74(16): 4671−4692.

[80] Aller R C. Sedimentary diagenesis, depositional environments, and benthic fluxes[M]//Holland H D, Turekian K K. Treatiseon Geochemistry. 2nd ed. Amsterdam: Elsevier, 2014: 293−334.

[81] Yao Wensheng, Millero F J. Oxidation of hydrogen sulfide by hydrous Fe(III) oxides in seawater[J]. Marine Chemistry, 1996, 52(1): 1−16.

[82] Böttcher M E, Thamdrup B. Anaerobic sulfide oxidation and stable isotope fractionation associated with bacterial sulfur disproportiona-

tion in the presence of MnO₂[J]. Geochimica et Cosmochimica Acta, 2001, 65(10): 1573−1581.

[83]　Schippers A, Jørgensen B B. Oxidation of pyrite and iron sulfide by manganese dioxide in marine sediments[J]. Geochimica et Cosmochimica Acta, 2001, 65(6): 915−922.

[84]　Schippers A, Jørgensen B B. Biogeochemistry of pyrite and iron sulfide oxidation in marine sediments[J]. Geochimica et Cosmochimica Acta, 2002, 66(1): 85−92.

[85]　Canfield D E, Thamdrup B. The production of ^{34}S-depleted sulfide during bacterial disproportionation of elemental sulfur[J]. Science, 1994, 266(5193): 1973−1975.

[86]　窦衍光, 蔡峰, 李军, 等. 末次冰盛期−全新世东海陆坡滑塌沉积的地质年代与沉积学证据[J]. 第四纪研究, 2020, 40(3): 704−711.
　　　Dou Yanguang, Cai Feng, Li Jun, et al. Geological ages and sedimentology proofs of landslide layers from Last Glacial Maximum to Holocene in continental slope of the East China Sea[J]. Quaternary Sciences, 2020, 40(3): 704−711.

[87]　Deyhle A, Kopf A. Deep fluids and ancient pore waters at the backstop: stable isotope systematics (B, C, O) of mud-volcano deposits on the Mediterranean Ridge accretionary wedge[J]. Geology, 2001, 29(11): 1031−1034.

[88]　Teichert B M A, Torres M E, Bohrmann G, et al. Fluid sources, fluid pathways and diagenetic reactions across an accretionary prism revealed by Sr and B geochemistry[J]. Earth and Planetary Science Letters, 2005, 239(1/2): 106−121.

[89]　Chao H C, You Chenfeng, Wang B S, et al. Boron isotopic composition of mud volcano fluids: Implications for fluid migration in shallow subduction zones[J]. Earth and Planetary Science Letters, 2011, 305(1/2): 32−44.

[90]　Yamaoka K, Hong E, Ishikawa T, et al. Boron isotope geochemistry of vent fluids from arc/back-arc seafloor hydrothermal systems in the western Pacific[J]. Chemical Geology, 2015, 392: 9−18.

[91]　Foster G L, Von Strandmann P A E, Rae J W B. Boron and magnesium isotopic composition of seawater[J]. Geochemistry, Geophysics, Geosystems, 2010, 11(8): Q08015.

[92]　Spivack A J, Edmond J M. Boron isotope exchange between seawater and the oceanic crust[J]. Geochimica et Cosmochimica Acta, 1987, 51(5): 1033−1043.

[93]　Spivack A J, Palmer M R, Edmond J M. The sedimentary cycle of the boron isotopes[J]. Geochimica et Cosmochimica Acta, 1987, 51(7): 1939−1949.

[94]　Hemming N G, Hanson G N. Boron isotopic composition and concentration in modern marine carbonates[J]. Geochimica et Cosmochimica Acta, 1992, 56(1): 537−543.

[95]　You C F, Spivack A J, Gieskes J M, et al. Boron contents and isotopic compositions in pore waters: a new approach to determine temperature induced artifacts—geochemical implications[J]. Marine Geology, 1996, 129(3/4): 351−361.

[96]　Brumsack H J, Zuleger E. Boron and boron isotopes in pore waters from ODP Leg 127, sea of Japan[J]. Earth and Planetary Science Letters, 1992, 113(3): 427−433.

[97]　Magenheim A J, Spivack A J, Michael P J, et al. Chlorine stable isotope composition of the oceanic crust: implications for earth's distribution of chlorine[J]. Earth and Planetary Science Letters, 1995, 131(3/4): 427−432.

[98]　Eggenkamp H G M, Kreulen R, Koster Van Groos A F, et al. Chlorine stable isotope fractionation in evaporites[J]. Geochimica et Cosmochimica Acta, 1995, 59(24): 5169−5175.

[99]　Ransom B, Spivack A J, Kastner M. Stable Cl isotopes in subduction-zone pore waters: implications for fluid-rock reactions and the cycling of chlorine[J]. Geology, 1995, 23(8): 715−718.

[100]　Spivack A J, Kastner M, Ransom B. Elemental and isotopic chloride geochemistry and fluid flow in the Nankai Trough[J]. Geophysical Research Letters, 2002, 29(14): 6-1−6-4.

Geochemical characteristics and indicative significance of pore water in the sediments of Okinawa Trough

Sun Chenghui [1, 2, 5]，Dou Yanguang [2, 3]，Zhao Jingtao [2, 4]，Sun Zhilei [2, 4]，Bai Fenglong [2, 4]，Cai Feng [2, 4]，Li Qing [2, 4]，Zhai Bin [2, 4]，Wang Libo [2, 4]，Zou Liang [2, 4]

(1. *Chinese Academy of Geological Sciences*, *Beijing* 100037, *China*; 2. *China Geological Survey Qingdao Institute of Marine Geology*, *Qingdao* 266237, *China*; 3. *Laboratory for Marine Geology*, *Pilot National Laboratory for Marine Science and Technology* (*Qingdao*), *Qingdao* 266237, *China*; 4. *Laboratory for Marine Mineral Resource*, *Pilot National Laboratory for Marine Science and Technology* (*Qingdao*), *Qingdao* 266237, *China*; 5. *China University of Geosciences* (*Beijing*), *Beijing* 100083, *China*)

Abstract: Through the analysis of the δ^{13}C, δ^{18}O, δ^{11}B, δ^{37}Cl isotopes and Cl⁻, SO$_4^{2-}$, K⁺, and Na⁺ ion index in the sedi-

ment pore water of the core GSW1 in the East China Sea outer Slope-Okinawa Trough, the changes of early diagenesis, fluid sources, migration and oxidation environment of sediments were discussed. The results show that the pore water dissolved inorganic carbon of the core GSW1 mainly comes from sea water and organic matter , the concentration of SO_4^{2-} decreases more gently with depth, and the concentration of Cl^- is much lower than seawater. The sulfate consumption in the surface sediments of this pore is mainly caused by organoclastic sulfate reduction (OSR) controlled, anaerobic oxidation of methane (AOM) occurs in deeper layers below 4 m. The H_2S produced by OSR diffuses upwards and is enriched and oxidized, which is the main factor that causes the 110−360 cm SO_4^{2-} content to not significantly decrease. The overall trend of pore water SO_4^{2-} concentration decreases with depth, indicating that the deposition environment of core GSW1 has gradually changed from an oxidizing and sub-oxidizing environment to a reducing environment. The vertical changes of $\delta^{11}B$ and $\delta^{37}Cl$ fluctuate greatly. On the one hand, they are affected by the degradation of organic matter in the early diagenesis stage, and they may also be related to the diffusion of pore fluid and sediment/pore water interaction.

Key words: sulfate reduction; fluid migration; isotope and ion concentration; pore water; East China Sea outer Slope-Okinawa Trough